Precise, Facile Initial Rate Measurements[†]

Qingxiu Tang and Thomas S. Leyh*

The Department of Microbiology and Immunology, Albert Einstein College of Medicine, 1300 Morris Park Ave, Bronx, New York 10461-1926

Received: June 16, 2010

Progress curve analysis has been used sparingly in studies of enzyme-catalyzed reactions due largely to the complexity of the integrated rate expressions used in data analysis. Using an experimental design that simplifies the analysis, the advantages and limitations of progress curve experiments are explored in a study of four different enzyme-catalyzed reactions. The approach involves relatively simple protocols, requires 20−25% of the materials, and provides 10- to 20-fold signal enhancements compared to analogous initial rate studies. Product inhibition, which complicates integrated rate analysis, was circumvented using cloned, purified enzymes that remove the products and draw the reaction forward. The resulting progress curves can be transformed into the equivalent of thousands of initial rate and [*S*] measurements and, due to the absence of product inhibition, are plotted in the familiar, linear double-reciprocal format. Allowing product to accumulate during a reaction produces a continuously changing substrate/product ratio that can be used as the basis for obtaining product inhibition constants and to distinguish among the three classical inhibition mechanisms. Algebraic models describing the double-reciprocal patterns obtained from such inhibition studies are presented. The virtual continuum of substrate concentrations that occurs during a progress curve experiment provides a nearly errorless set of relative concentrations that results in remarkably precise data; kinetic constant standard deviations are on the order of 0.5%.

Introduction

Initial rate studies of enzyme-catalyzed reactions are an experimental mainstay of biochemical science. The constants obtained from these studies have been used in a myriad of creative ways to explore and define the functional properties of enzymes and their interactions with biological and synthetic effectors. Elegant, powerful rules governing the design and interpretation of initial rate experiments, including inhibition studies, have provided an invaluable template for these investigations for four decades.[1–3] Progress curve analysis is a less familiar means of obtaining similar constants that, as is shown below, offers several advantages over the initial rate approach; first, it provides an approximate 20-fold increase in signal because the data used to obtain the kinetic constants spans the entire range of the reaction (0−100%) rather than the first ∼5%. Second, the method does not require the preparation of multiple samples to study a range of substrate concentrations; a virtual continuum of substrate concentrations is generated during the course of a single reaction, resulting in a considerable savings of time and materials and remarkably precise data.

A drawback of the progress curve approach is that kinetic constants are obtained by statistically fitting data to integrated rate equations that are complex[4–6] and do not lend themselves to the intuitive interpretations that draw naturally from the linear patterns associated with initial rate data when it is presented in double-reciprocal form (i.e., 1/[*S*] vs 1/[v]). A second drawback is that the product produced during the progress curve experiment inhibits the reaction, complicating the interpretation. By determining the instantaneous velocity and substrate concentration throughout a progress curve, the curve can be transformed into what is tantamount to thousands of individual initial rate and substrate concentration measurements that can be cast in double-reciprocal form to yield the familiar linear patterns. The product inhibition problem can be circumvented using cloned, purified enzymes that remove the products and thermodynamically draw the reaction forward. Alternatively, if product is allowed to accumulate, a continuously varying substrate/product inhibitor ratio develops during the reaction that, when plotted in double-reciprocal format, results in patterns that can be used to assign the type of inhibition. These and other issues are discussed in this article, which explores the advantages and limitations of double-reciprocal progress curves in a study of four different enzyme-catalyzed reactions.

Materials and Methods

The materials and suppliers used in this study are as follows. NADH, $NADP^+$, ATP, ADP, AMP, GTP, phospho(enol)pyruvate (PEP), and glucose were purchased from the Sigma Chemical Co. 2-Amino-6-mercapto-7-methylpurine riboside (MESG) and purine nucleoside phosphorylase (PNP) were purchased from Molecular Probes. Inc. Pyruvate kinase (rabbit muscle), hexokinase (yeast), lactate dehydrogenase (rabbit muscle), and glucose-6-phosphate dehydrogenase (yeast) were purchased from Roche Applied Science. Salts and buffers were of the highest grades available from Fisher Scientific. Phosphomevalonate was synthesized and purified as described previously.[7] ATP sulfurylase (*E. coli*), phosphomevalonate kinase (*S. pneumoniae*), and diphosphomevaloante decarboxylase (*S. pneumoniae*) were expressed and purified as described previously.[7–9]

Preparation and Preliminary Characterization of the Enzymes. All of the enzymes, including coupling enzymes, were dialyzed extensively against Hepes/K^+ (50 mM, pH =

[†] Part of the "Robert A. Alberty Festschrift".

* To whom correspondence should be addressed. Phone: 718-430-2857. Fax: 718-430-8565. E-mail: leyh@aecom.yu.edu.

10.1021/jp1055528
Published on Web 08/24/2010

8.0), and the specific activity of each enzyme was determined in the buffer used in the rate studies (i.e., Hepes/K^+ (50 mM, pH = 8.0)).

Initial Rate Measurements. Initial rates were measured at four substrate concentrations, equally spaced in reciprocal space, that ranged from 0.50 to 6.3K_m in the phosphomevalonate kinase study (ATP = 5.0 mM, 36K_m) and from 1.4 to 14K_m in the pyruvate kinase study (ATP = 0.50 mM, 3.7K_m). Rate measurements were taken during consumption of less than the first 8% of the concentration-limiting substrate. The thermodynamic bias of the systems, including coupling enzymes, was sufficient to draw essentially 100% of the concentration-limiting substrate to product. The coupling enzyme V/K_m values were set such that the coupled reactions achieved steady state in <15 s.[10] Measurements were made in triplicate, and the data were fit using the weighted least-squares program of Cleland.[11]

Progress Curves and Data Analysis. Reactions were performed in triplicate, at 5000−10000 data points/curve. Then, 5−95% of the reaction region of the progress curves was analyzed. The velocity was calculated at each point in the curve by determining the slope from a set of points that was centered on the point of interest and that spanned ±0.5% of the total data set; the concentration associated with that same point was obtained by averaging the concentrations over the identical span. Reducing the size of the filter below ±0.5% (i.e., 1%) did not significantly affect the value of the slope or concentration; effects were observed above ~1.5%. The data were then plotted in double-reciprocal format (1/[S] vs 1/[v]), and the linearity of the data was optimized by making tiny adjustments (typically less than 1%) in the initial concentration of the substrate used in the calculations. Data sets collected under identical conditions were combined and averaged using a Fortran 77 program written for this purpose (available upon request). The program averages the progress curve that it parses into a user-defined number (typically 200−500) of contiguous, equally spaced intervals that span the experimental concentration range. The averaged data is then fit using the Cleland algorithms, which were modified to accept data sets containing more than 100 velocity/substrate records by increasing the dimension of the velocity and substrate variables. The reactions were monitored using a Cary 100 or 400 UV/vis spectrophotometer.

Results and Discussion

Varying a Single Substrate: Phosphomevalonate Kinase. Phosphomevalonate kinase (ATP/5-phosphomevalonate phosphotransferase, E.C. 2.7.4.2) catalyzes transfer of the γ-phosphoryl group of ATP to the 1-phosphate of phosphomevalonate to form the pyrophosphoryl linkge found in diphosphomevalonate and ADP (reaction 1).

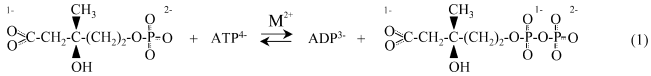

(1)

A divalent cation is required for catalysis, and K_{eq} = 7.8 (pH = 8.0, Mg^{2+} = [nucleotide] + 1.0 mM, T = 25 °C[7]). Reaction 1 is an essential step in isoprenoid biosynthesis in mammals, archea, and certain bacteria, including *Streptococcus pneumoniae*, the bacterium from which the enzyme used in the current studies was cloned.[12] The enzyme is a member of the GHMP kinase superfamily, which is recognizable, in part, by a unique architecture surrounding the γ-phosphoryl group that has been structurally, but not functionally, well-defined.[13,14]

The phosphomevalonate kinase assay used in the progress curve study was designed to prevent product inhibition and draw the reaction forward by continuous removal of both reaction products ADP and dipohosphomevalonate. ADP was removed using the well-described pyruvate kinase/lactate dehydrogenase system,[15] which regenerates ATP from ADP and stoichiometrically (1:1) oxidizes NADH, which provides the optical change used to monitor the reaction ($\Delta\varepsilon^*_{340}$ = 6.22 mM^{-1} cm^{-1}). Diphosphomevalonate was removed using the enzyme diphosphomevalonate decarboxylase (ATP/(R)-5-diphosphomevalonate carboxy-lyase, E.C. 4.1.1.33), which was expressed and purified for this purpose (see Materials and Methods). Diphosphomevalonate decarboxylase catalyzes the decarboxylation of diphosphomevalonate and the hydrolysis of ATP to yield isopentenyl diphosphate, CO_2, ADP, and P_i. The ADP produced in the decarboxylation reaction is linked by the pyruvate kinase/lactate dehydrogenase system to the oxidation of a second NADH. The equilibrium constants associated with the coupled reactions, in the direction used in the assay, are as follows: pyruvate kinase (K_{eq} = 6.5 × 10^4 (pH = 7.0, 30 °C)[16]), lactate deyhdrogenase (K_{eq} = 3.7 x10^6, (pH = 7.0, 25 °C)[17]), and diphosphomevalonate decarboxylase (considered irreversible[18]). Given the very favorable energetics of these reactions, the phosphomevalonate kinase reaction was treated as if 100% of the concentration-limiting substrate (phosphomevalonate) was consumed; the ΔOD^s associated with the overall reactions confirmed that this was the case.

Results obtained from the progress curve (continuous line) and initial rate (open circles) studies of the PMK system are compared in Figure 1. The lowest PM concentration used in the initial rate experiment was 7.7 μM. Conversion of 5% of phosphomevalonate at 7.7 μM corresponds, in this assay, to a ΔOD_{340} of 0.0046. Measuring this small of a change in OD is technically challenging and represents a reasonable lower detection limit for an excellent UV/vis instrument. It is notable that this entire OD range is not accessible to the experimentalist due to substrate losses that occur during mixing and the lag time needed to reach the steady state. In contrast, the progress curve reciprocal velocity is linear to a phosphomevaloante concentration of 670 nM, a 12-fold decrease in the lower limit of detection compared to the initial rate method. A close-up of the initial rate region of the plot demonstrates that the two methods agree well and that the error in the progress curve data is quite small compared to that seen in the initial rate data. The data were fit using the Hypero program developed by Cleland.[11] The best-fit parameters associated with the initial rate and progress curve approaches are, respectively, $K_{m(app)}$ = 13 (±1.1), $V_{m(app)}$ = 5.91 (±0.17) and $K_{m(app)}$ = 15.9 (±0.045), $V_{m(app)}$ = 6.67 (±0.012). The constants obtained from the two approaches are similar, validating the progress curve approach; however, their precision is not. Standard deviations in the initial rate constants range from 2.9 to 8.5%, while those associated with the progress curve constants range from 0.18 to 0.28%. The remarkable sensitivity and small error associated with the progress curve data are due to the essentially errorless change in substrate concentration that occurs during the reaction because the concentration is changed in situ by a molecular process that generates a virtual continuum of substrate concentrations, there are no volume errors, and the cuvette is not moved.

Varying Two Substrates: Hexokinase and Pyruvate Kinase. Hexokinase (ATP/D-hexose 6-phosphotransferase, E.C. 2.7.1.1) and pyruvate kinase (ATP/pyruvate 2-O-phosphotrans-

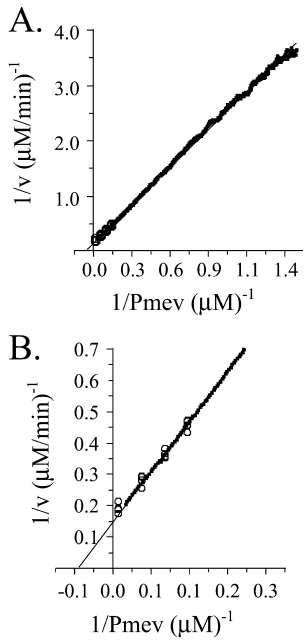

Figure 1. Initial rate and double-reciprocal progress curve studies of the phosphomevalonate kinase reaction. (A) Double-reciprocal plot of the data obtained using both methods. The thick, solid line represents a progress curve in which phosphomevalonate is consumed and [ATP] is held fixed at 5.0 mM using a regenerating system. The open circles represent the results of a study in which initial rates were obtained at each of four phosphomevalonate concentrations (100, 20, 11, and 7.7 μM); [ATP] = 5.0 mM ($36K_m$). Straight lines through the data represent the behavior predicted by the best-fit parameters (see Table 1) obtained from a weighted fit of the progress curve data to a sequential model (see Materials and Methods). Experiments were performed in triplicate. The assay composition and conditions were as follows: phosphomevalonate kinase (0.05 μM), phosphomevalonate decarboxylase (0.60 U/ml), lactate dehydrogenase (10 U/ml), pyruvate kinase (25 U/ml), phosphomevalonate (0.08 mM), ATP (5.0 mM), PEP (1.0 mM), NADH (0.30 mM), $MgCl_2$ (6.0 mM), KCl (50 mM), Hepes (50 mM, pH = 8.0/K^+), $T = 25 \pm 2$ °C. The reactions were monitored at 339 nm and initiated by addition of phosphomevalonate kinase. Data processing is described in Materials and Methods. (B) Close-up of the initial rate results.

TABLE 1: Double-Reciprocal Progress Curve Kinetic Constants

pyruvate kinase	hexokinase
V_m = 58.4 (0.063)[a]	V_m = 204 (0.46)
$K_{m\,(PEP)}$ = 14.2 (0.032) μM	$K_{m\,(Glu)}$ = 400 (1.7) μM
$K_{m\,(ADP)}$ = 135 (0.36) μM	$K_{m\,(ATP)}$ = 29.5 (0.58) μM
$K_{i\,(PEP)}$ = 11.1 (0.049) μM	$K_{i\,(Glu)}$ = 3280 (66) μM
$K_{i\,(ADP)}$ = 106 (0.39) μM	$K_{i\,(ATP)}$ = 241 (1.0) μM

[a] Standard errors are given in parentheses.

ferase, 2.7.1.40) are well-studied glycolytic enzymes that catalyze reactions 2[19–21] and 3,[22–24] respectively.

$$ATP^{4-} + \text{D-glucose} \overset{Mg^{2+}}{\rightleftharpoons} ADP^{3-} + \text{D-glucose-6-phosphate}^{2-} + H^+ \quad (2)$$

$$ADP^{3-} + PEP^{3-} + H^+ \overset{Mg^{2}}{\underset{K^+}{\rightleftharpoons}} ATP^{4-} + \text{pyruvate}^- \quad (3)$$

These enzymes are often used in coupling schemes to monitor kinase reactions because they regenerate the nucleotide substrate

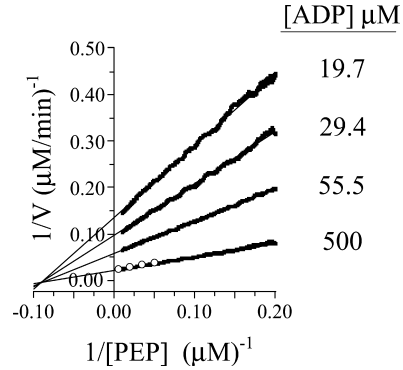

Figure 2. Initial rate and double-reciprocal progress curve study of the pyruvate-kinase-catalyzed reaction. Thick, solid lines represent progress curves in which PEP was consumed and ADP was held fixed, at the four concentrations indicated, using a regenerating system. Open circles represent the results of initial rate measurements taken at four different concentrations of PEP (200, 50, 29, and 20 μM); [ADP] = 500 μM ($3.7K_m$). The lines through the data represent the behavior predicted by the best-fit constants (see Table 1) obtained from a weighted fit of the progress curve data to a model for a sequential mechanism (see Materials and Methods). The composition and conditions of the assay were as follows: pyruvate kinase (0.030 U/ml), hexokinase (4.8 U/ml), lactate dehydrogenase (2.0 U/ml), ADP (at the indicated concentrations), PEP (0.20 mM), NADH (0.30 mM), glucose (1.0 mM), KCl (100 mM), $MgCl_2$ (2.0 mM), Hepes (50 mM, pH = 8.0/K^+), $T = 25 \pm 2$ °C. The reactions were initiated by the addition of ATP and monitored at 339 nm. Experiments were performed in triplicate.

of the primary enzyme and produce a product that can be linked, using a dehydrogenase, to the oxidation or reduction of a nicotinamide adenine dinucleotide, which provides an optical signal for turnover

The assay used to monitor the pyruvate-kinase-catalyzed reaction removed both of the products, ATP and pyruvate, using hexokinase and lactate dehydrogenase. The ADP consumed in the puruvate kinase reaction is regenerated by the hexokinase reaction, and pyruvate is removed and coupled to the oxidation of NADH by lactate dehydrogenase. The glucose-6-phosphate concentration was held in excess over PEP, which ensured that ADP, the fixed-variable substrate, was held at its initial concentration throughout the progress curve (see Figure 2 legend).

The result of double-reciprocal progress curve study at four different ADP concentrations is shown in Figure 2. The straight lines passing through the data represent the behavior predicted by the best-fit constants obtained from the Sequeno program,[11] which uses a $(1/v)^4$ weighting to fit the data to an algebraic model for a simple sequential mechanism. The data and model agree with a precision that is nearly impossible to achieve using standard-practice initial rate techniques; the kinetic constant standard errors range from 0.11 to 0.44% (Table 1). To demonstrate that the progress curve and initial rate methods yield similar results, initial rate measurements were made, using assay conditions identical to those for the progress curve, at four different PEP concentrations; ADP was held fixed at 500 μM (i.e., the highest concentration used in the progress curve experiment). The result, represented by the open circles in Figure 2, confirms that the methods agree well. The initial rate study was performed in triplicate and required the preparation of 12 separate assay solutions. The analogous progress curve experiment required only three solutions and thus offers a considerable savings in time and reagents. The lowest PEP concentration used in the initial rate experiment, 20 μM, is a reasonable lower limit for what can be detected using this method (5% of 20 μM

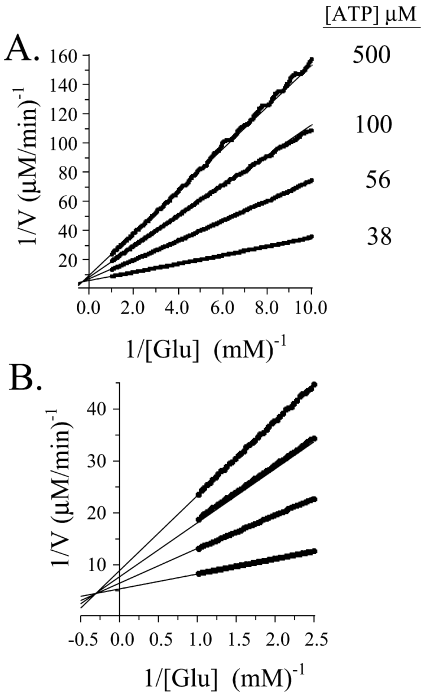

Figure 3. Double-reciprocal progress curve study of the hexokinase-catalyzed reaction. (A) The thick, solid lines represent progress curves in which glucose is consumed and ADP is held fixed, at the concentrations indicated, using a regenerating system. The lines through the data represent the behavior predicted by the best-fit parameters (see Table 1) obtained from a weighted, least-squares fit to a model for a sequential mechanism (see Materials and Methods). The experiments were performed in triplicate and averaged. The composition and conditions of the assay were as follow: hexokinase (0.030 U/ml), pyruvate kinase (4.0 U/ml), glucose-6-phosphate dehydrogenase (6.0 U/ml), glucose (1.5 mM), ATP (at the concentrations indicated), $NADP^+$ (1.8 mM), PEP (2.0 mM), $MgCl_2$ (1.5 mM), Hepes (50 mM, pH = 8.0/K^+), $T = 25 \pm 2$ °C. The detection wavelength, 390 nm, was shifted away from the absorbance maximum to avoid high background. (B) The point of intersection.

corresponds to a ΔOD_{340} of 0.00622). As can be seen, the progress curves provide excellent rate measurements at PEP concentrations as low as 5 μM (lower concentrations are readily achievable).

The hexokinase reaction poses a technically challenging problem for initial rate studies because the synergy in the binding reactions places the point-of-intersection of the 1/[*S*] versus 1/v curves so near the 1/v axis that it is difficult to position it well enough to determine whether it lies on or off of the 1/v axis, an issue that can be critical in assigning a mechanism. This problem caused considerable debate regarding whether the binding of ATP and glucose is random or ordered in the hexokinase mechanism;[25–28] the issue was ultimately resolved — binding is random.[28–30]

The result of a progress curve study of the hexokinase reaction is shown in Figure 3. ADP was removed, and ATP was regenerated by the pyruvate kinase reaction. Glucose-6-phosphate was removed and coupled to the reduction of $NADP^+$ using glucose-6-phophate dehydrogenase. PEP was in excess over glucose, which was consumed during the reaction, and ATP was held fixed at its initial concentration by the regenerating system. The straight lines through the data represent the behavior predicted by the best-fit parameters obtained from the Sequeno program.[11] The hexokinase data are well-described by the sequential model; the standard errors in the kinetic constants are comparable to those seen in the pyruvate kinase study (Table 1). That the intersection point is near the 1/v axis is well illustrated in panel A. To more closely inspect the relationship of the point-of-intersection and 1/v axis, the plot was magnified in the vicinity of the point (Figure 3B). The data argue far more convincingly for an off-axis point-of-intersection than traditional initial rate studies would allow and provide strong opposition to an equilibrium ordered mechanism. Thus, the progress curve approach can prove particularly valuable in cases where interpretation pivots on precision.

Product Inhibition: ATP Sulfurylase-GTPase. When product is allowed to accumulate, a continuously changing substrate/product ratio forms during the experiment. This ratio changes in a predictable way and provides the basis for product inhibition studies. Equation 4 describes a simple competitive inhibition scheme in which ligand binding is at equilibrium during steady-state turnover.

Competitive:

$$1/v = (K_m/V_m + K_m[I]/K_i \cdot V_m)1/[S] + 1/V_m \quad (4)$$

$$1/v = (K_m/V_m + K_m([I]_o + [S]_o)/K_i \cdot V_m)1/[S] + (1 - K_m/K_i) \cdot 1/V_m \quad (5)$$

The model predicts linear 1/[*S*] versus 1/v plots that intersect at 1/V_m at all fixed-variable concentrations of [*I*] (i.e., the well-know competitive inhibition pattern). The model is readily modified to describe the analogous progress curve using the substitution $[I] = [I]_o + [S]_o - [S]$ ([*I*] and [*S*] are instantaneous concentrations; $[I]_o$ and $[S]_o$ are concentrations at $t = 0$). The resulting progress curve formula, eq 5, also predicts linear 1/[*S*] versus 1/v plots that intersect on the 1/v axis; however, the intersection point, which is given by $(1 - K_m/K_i) \cdot 1/V_m$, can be positive or negative, depending on K_m/K_i.

The double-reciprocal progress curve pattern associated with a competitive inhibition system was experimentally demonstrated using the GTPase reaction catalyzed by ATP sulfurylase (ATP/sulfate adenylyltransferase, E.C. 2.7.7.4), from *E. coli* K−12. ATP sulfurylase catalyzes and conformationally couples the energetics of two, separate reactions, the synthesis of adenosine-5′-phosphosulfate (APS, or activated sulfate) and the hydrolysis of GTP (reactions 6 and 7, respectively).[31,32]

$$ATP^{4-} + SO_4^{2-} \rightleftarrows APS^{2-} + P_2O_7^{4-} \quad (6)$$

$$GTP^{4-} + H_2O \rightleftarrows GDP^{3-} + HPO_4^{2-} + H^+ \quad (7)$$

The GTPase reaction is allosterically activated by AMP, which binds at the ATP binding site.[8] AMP binding is believed to elicit an enzyme form that mimics an intermediate stage of the native reaction in which the α,β-bond of ATP has been cleaved. Initial rate studies have demonstrated that GDP is a competitive inhibitor versus GTP in this reaction.[31]

The inhibition study was performed at three different initial GTP concentrations (45, 30, or 15 μM), and GDP accumulated during the reactions. Progress of the reactions was monitored using the purine nucleoside phosphorylase (PNP)−MESG system. Purine nucleoside phosphorylase (purine nucleoside/orthophosphate ribosyltransferase, E.C. 2.4.2.1) catalyzes cleavage of the *N*-glycosidic bond of MESG (2-amino-6-mercapto-7-methylpurine riboside) to yield ribose-1-phosphate and 2-amino-6-mercapto-7-methylpurine (reaction 8). Cleavage results in a

pH-dependent change in absorbance that can be used to monitor phosphate release.

$$\text{MESG} + \text{HPO}_4^{2-} \rightleftarrows \text{ribose-1-phosphate}^{2-} + \text{2-amino-6-mercapto-7-methylpurine} \quad (8)$$

A standard curve that normalized the change in absorbance and phosphate concentration was constructed. The curve was linear in phosphate concentration to 70 μM, and $\Delta\varepsilon^*_{360} = -7.0\ \text{mM}^{-1}\ \text{cm}^{-1}$. The data were fit using the Compo program of Cleland.[11] As predicted by the algebra, the $1/[S]$ versus $1/v$ plots are linear. Once again, the experiments were quite simple to perform, and the best-fit constants obtained from the data analysis were remarkably precise, $K_m = 30.1$ ($\pm$0.37), $K_{is} = 17.2$ ($\pm$0.15), and $V_m = 42.4$ ($\pm$0.34).

Algebraic models describing the double-reciprocal progress curve patterns associated with simple uncompetitive (I binds ES) and noncompetitive (I binds E and ES) inhibition are derived from their initial rate predecessors using the substitution described above for competitive inhibition (eqs 9−12).

Uncompetitive:

$$1/v = (K_m/V_m) \cdot 1/[S] + (1 + [I]/K_{is}) \cdot 1/V_m \quad (9)$$

$$1/v = (K_m/V_m) \cdot 1/[S] + (1 + [I]_o/K_{is} + ([S]_o - [S])/K_{is} - K_m/K_i) \cdot 1/V_m \quad (10)$$

Noncompetitive:

$$1/v = (K_m/V_m + K_m[I]/K_i \cdot V_m) \cdot 1/[S] + (1 + [I]/K_{is}) \cdot 1/V_m \quad (11)$$

$$1/v = (K_m/V_m + K_m([I]_o + [S]_o)/K_i \cdot V_m) \cdot 1/[S] + (1 + [\text{I}]_o/K_{is} + [S]_o/K_{is} - K_m/K_i) \cdot 1/V_m - [S]/K_{is} \cdot V_m \quad (12)$$

In both cases, the factors preceding $1/V_m$ are identical (i.e., $1 + [I]_o/K_{is} + ([S]_o - [S])/K_{is} - K_m/K_i$); they are rectangular hyperbolas in double-reciprocal space that plateau as $[S]$ becomes small compared to $[S]_o$. The two patterns are distinguishable on the basis of the differences in the factors that precede $1/[S]$. The noncompetitive $1/[S]$ factor depends linearly on the sum $[I]_o + [S]_o$, whereas this same factor is independent of these concentrations in the uncompetitive model. The differences are most pronounced at the early stages of the reactions where the $1/V_m$ factor is minimized because $[S] \approx [S]_o$. For a plot of the ATP sulfurylase-catalyzed hydrolysis of GTP, see Figure 4.

Conclusions

The progress curve protocols described in this article are simple, efficient, and provide remarkably precise data. The sensitivity is 10 to 20 times that of the analogous initial rate experiment, which, in favorable cases, results in a comparable decrease in the lower limit of K_m and/or K_i that can be determined using a given detection method. It is shown that a single progress curve can be processed to yield the equivalent of thousands of initial rate measurements that can be plotted in double-reciprocal format to obtain the standard, linear $1/[S]$ versus $1/v$ patterns. An experiment in which the product is allowed to accumulate (i.e., one in which a continuously varying substrate/product ratio occurs) can be used to obtain product inhibition constants and to distinguish among the three well-known inhibition mechanisms, competitive, noncompetitive, and uncompetitive. On balance, double-reciprocal progress curves have proven to be a facile, hyperprecise means of extracting kinetic constants from rate data that offers significant technical advantages over initial rate measurements.

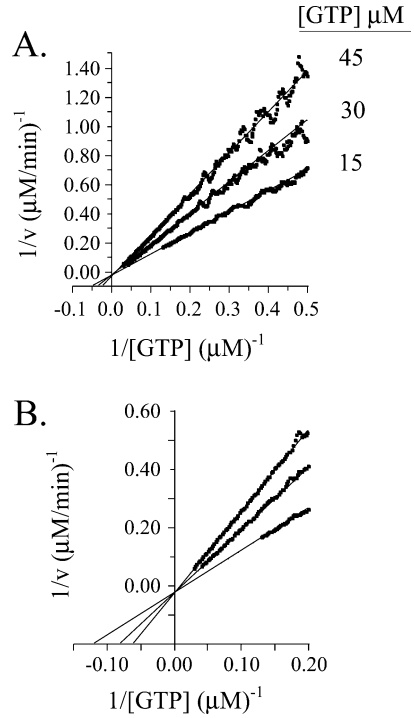

Figure 4. Competitive product inhibition study: the ATP sulfurylase-catalyzed hydrolysis of GTP. (A) The thick, solid lines represent progress curves in which GTP is consumed and GDP, a competitive inhibitor, is allowed to accumulate. Lines through the data represent the behavior predicted by the best-fit parameters obtained from a weighted fit to a competitive inhibition model (see Materials and Methods). Phosphate was removed, and the optical signal used to monitor the reaction was generated using purine nucleoside phosphorylase with MESG as a substrate. The experiments were preformed in triplicate and averaged. The composition and conditions of the assay were as follows: ATP sulfurylase (0.50 μM), purine nucleoside phosphorylase (1.0 U/ml), GTP (at the concentrations indicated), MESG (0.90 mM), $MgCl_2$ (3.0 mM), AMP (2.0 mM), $T = 25 \pm 2$ °C. The reactions were initiated by addition of ATP sulfurylase and monitored at 360 nm. (B) The $1/v$ axis close-up.

Acknowledgment. We would like to thank Dr. S. Chandra Shekar, a postdotdoctoral fellow in Dr. Mark Girvin's laboratory at the Albert Einstein College of Medicine, for his help in writing the Fortran 77 program. This work was supported by the National Institutes of Health Grant GM54469.

References and Notes

(1) Cleland, W. W. *Biochim. Biophys. Acta* **1963**, *67*, 104–137.
(2) Cleland, W. W. *Biochim. Biophys. Acta* **1963**, *67*, 173–187.
(3) Cleland, W. W. *Biochim. Biophys. Acta* **1963**, *67*, 188–196.
(4) Boeker, E. A. *Biochem. J.* **1984**, *223*, 15–22.
(5) Schiller, M. R.; Holmes, L. D.; Boeker, E. A. *Biochim. Biophys. Acta* **1996**, *1297*, 17–27.
(6) Duggleby, R. G.; Wood, C. *Biochem. J.* **1989**, *258*, 397–402.
(7) Pilloff, D.; Dabovic, K.; Romanowski, M. J.; Bonanno, J. B.; Doherty, M.; Burley, S. K.; Leyh, T. S. *J. Biol. Chem.* **2003**, *278*, 4510–4515.
(8) Wei, J.; Leyh, T. S. *Biochemistry* **1998**, *37*, 17163–17169.
(9) Bonanno, J. B.; Edo, C.; Eswar, N.; Pieper, U.; Romanowski, M. J.; Ilyin, V.; Gerchman, S. E.; Kycia, H.; Studier, F. W.; Sali, A.; Burley, S. K. *Proc. Natl. Acad. Sci. U.S.A.* **2001**, *98*, 12896–12901.
(10) McClure, W. R. *Biochemistry* **1969**, *8*, 2782–2786.
(11) Cleland, W. W. *Methods Enzymol.* **1979**, *63*, 103–138.

(12) Romanowski, M. J.; Bonanno, J. B.; Burley, S. K. *Proteins* **2002**, *47*, 568–571.
(13) Bork, P.; Sander, C.; Valencia, A. *Protein Sci.* **1993**, *2*, 31–40.
(14) Tsay, Y. H.; Robinson, G. W. *Mol. Cell. Biol.* **1991**, *11*, 620–631.
(15) Buchler, T.; Pfleiderer, G. In *Methods in Enzymology*; Colowick, S. P., Kaplan, N. O., Eds.; Academic Press: New York, 1955; Vol. 1, pp 435−440.
(16) McQuade, J.; Utter, M. *J. Biol. Chem.* **1959**, *234*, 2151–2157.
(17) Hakala, M.; Glais, A.; Schwert, G. *J. Biol. Chem.* **1956**, 191–209.
(18) Barman, T. E. *Enzyme Handbook*; Springer-Verlag: New York, 1969.
(19) Jones, J. P.; Weiss, P. M.; Cleland, W. W. *Biochemistry* **1991**, *30*, 3634–3639.
(20) Viola, R. E.; Raushel, F. M.; Rendina, A. R.; Cleland, W. W. *Biochemistry* **1982**, *21*, 1295–1302.
(21) Wilkinson, K. D.; Rose, I. A. *J. Biol. Chem.* **1979**, *254*, 12567–12572.
(22) Larsen, T. M.; Laughlin, L. T.; Holden, H. M.; Rayment, I.; Reed, G. H. *Biochemistry* **1994**, *33*, 6301–6309.
(23) Larsen, T. M.; Benning, M. M.; Rayment, I.; Reed, G. H. *Biochemistry* **1998**, *37*, 6247–6255.
(24) Bollenbach, T. J.; Nowak, T. *Biochemistry* **2001**, *40*, 13097–13106.
(25) Fromm, H.; Zewe, V. *J. Biol. Chem.* **1962**, *237*, 3027–3032.
(26) Hammes, G. G.; Kochavi, D. *J. Am. Chem. Soc.* **1962**, *84*, 2069–2073.
(27) Hammes, G. G.; Kochavi, D. *J. Am. Chem. Soc.* **1962**, *84*, 2073–2076.
(28) Rudolph, F. B.; Fromm, H. J. *J. Biol. Chem.* **1971**, *246*, 6611–6619.
(29) Ning, J.; Purich, D. L.; Fromm, H. J. *J. Biol. Chem.* **1969**, *244*, 3840–3846.
(30) Solomon, F.; Rose, I. A. *Arch. Biochem. Biophys.* **1971**, *147*, 349–350.
(31) Liu, C.; Suo, Y.; Leyh, T. S. *Biochemistry* **1994**, *33*, 7309–7314.
(32) Wei, J.; Leyh, T. S. *Biochemistry* **1999**, *38*, 6311–6316.

JP1055528